Impedance Spectroscopy for Microfluidic Particle-analyzing Device with Spatial-Coplanar Electrode Design

Ting-Wei Wu, Chia-Hong Gao, Fan-En Chen, Chih-Ting Lin
Graduate Institute of Electronics Engineering, National Taiwan University, Taipei 10617, Taiwan (R.O.C.)
r04943173@ntu.edu.tw; r03943068@ntu.edu.tw; timlin@ntu.edu.tw

***Abstract*—In this work, we present a new microfluidic particle-analyzing device with a spatially coplanar-electrode design. To achieve effective particle analysis, 4 coplanar electrodes were designed and fabricated on glass substrates. Different from traditional cross-channel electrodes in impedance sensing, the coplanar design can be achieved without precise alignment issue, which is the major obstacle of traditional designs. Then, to characterize impedance spectroscopy of the device, a frequency spectrum of fabricated device impedance is employed. Based on the experimental results, theoretically simulated impedance behaviors are clearly compatible with experiments measured by fabricated devices. With different size of polystyrene beads (3, 6, 10 um) flowing through a set of 20um scale electrodes, we have experimentally demonstrated fabricated device's capabilities of differentiating bead sizes and positions due to resonance characteristics at the chosen frequency, 1 MHz. In addition, stray capacitance effect, well-known to deteriorate the detection of signals from bead flows, would be influenced and ameliorated by substrate material selection. This effect has also been discussed in this work on frequency analysis and simulation as well.**

Keywords—Microfluidics; Electrode Design; Impedance; Flow Cytometry; Particle Analysis

I. INTRODUCTION

Single cell impedance cytometry offers low cost and label-free cell analysis compared with traditional flow cytometry method. In 2001, Renaud *et al* proposed the first microfluidics-based impedance cytometer [1], which was with a set of co-planar electrode. Then, Renaud *et al* further proposed a set of parallel electrodes with plate face-to-face alignment [2] so as Morgan in 2011 considering z-positional dependence of particles in two sets of parallel electrodes [3]. However, misalignment issues would significantly affect the device's performance and increase the fabrication complexity. Further, AC impedance sensing is limited to a frequency range influenced by double layer impedance and parasitic behavior, as the first addressed by gold micro electrodes [4] and platinum electroplated ones [5]. The latter stray capacitance effect will also significantly thwart the operational frequency range extension to higher level above 10MHz.

So, in present work, a novel coplanar electrode is spatially designed and implemented on a glass substrate. To characterize the fabricated devices, the non-linear electrical field issue is addressed by flow rate control [6]. Then, a frequency range, i.e. 1 MHz to 10 MHz, is simulated out from an impedance spectrum and manifests the optimal sensing area for particle analyzing where non-ideal capacitance effects do not dominate. The signal response measurements at this frequency range are agreed with a proposed electrical model and an operational frequency at 1MHz can be then determined to have capabilities in bead differentiation. In addition, stray capacitance effect is then demonstrated and addressed under COMSOL simulation for further work.

II. EXPERIMENT

A. Fabrication Process

The particle-analyzing device can be fabricated as shown in the previous work [6]. To elaborate on, there are mainly two fabrication procedures: Microfluidic channel and Planar electrode fabrications. SU8-2005 photoresists (MicroChem Corp., MA, USA) are spun on a silicon wafer with 410 rpm for 40s where 15um channel height is then defined. Afterwards, Photolithography determines the channel pattern on the silicon mode which the polydimethylsiloxane (PDMS) is poured and cured on. Defined PDMS microfluidic channel will be peeled from the mode and bounded on an oxygen-plasma treated glass substrate with the planar electrodes, which are evaporated by 20 nm chromium and 50 nm gold. The electrode design is defined by four 20 um width thin-film Au/Cr electrode geometry with a pitch of 20 um as shown in Fig. 1a. To obtain particle position/size information, the 4 electrodes are grouped as across (A-C) and neighbor (A-B) for multi-signal comparison. At the same time, referring to the distance of beads from the electrode A which is applied 1V AC signal, three position differentiation regions, i.e. far, center, near regions, of bead position are indicated as shown in Fig. 1b. The entire particle-analyzing device is shown in Fig. 2. and 300mM Potassium Chloride (KCL) solution is used as electrolyte and medium for particle analyzing.

B. Impedance Analysis

Inside our particle-analyzing device, a newly developed-modified electrical model considering channel ambience has been established as shown in Fig. 3 [5,7]. The channel impedance R_{SOL} is in series with a set of constant phase elements from double layer impedances, produced by the metal-electrode interface. This series metal-electrolyte impedance is inversely proportional to the electrode surface area where small-scaling could inevitably reduce the sensor sensitivity [4,8]. However, higher applied frequency could significantly abate the double layer impedance effect and will show relatively better sensing ability for channel impedance. Unfortunately, the stray capacitance C_{st}, which is the generic unwanted coupling capacitance between four electrodes, impose an upper limit of the operational frequency [9]. It will violate the device's sensitivity of particles' intracellular

properties under high operational frequency. So to study AC impedance sensing, a frequency range limits device capability of detecting flowing particles. Therefore, in our work, this frequency range is further specified particularly for the designed device under a simulated impedance result. The impedance spectrum is able to provide information on the influence of double layer impedance and non-ideal capacitance effects in the microchannel.

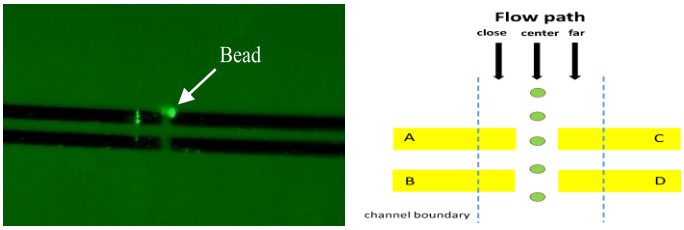

(a) (b)

Fig. 1. (a) Micrograph of four electrode geometry under fluorescence with 10um bead indicated and (b) 4 electrodes are defined A, B, C, D and for differentiation use, bead are set as near, center, far positions.

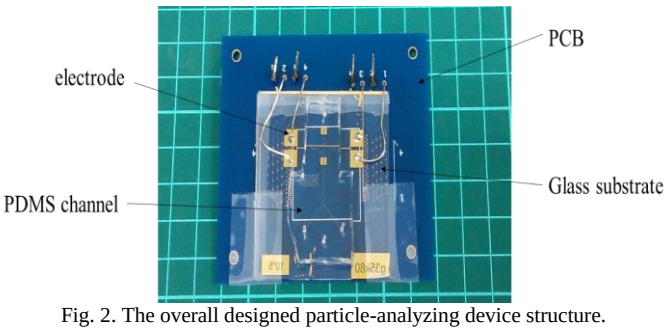

Fig. 2. The overall designed particle-analyzing device structure.

Under the required frequency range, a cell model is further introduced into the microchannel ambience. The electrical properties of different cellular structures could be basically modeled as Cell membrane capacitance C_c in series with Cytoplasm resistance R_c. They both possess conductivity and permittivity, the ability to conduct or store charges respectively when an electrical field is applied. A phenomenon called dispersion occur when increasing applied frequencies lower the permittivity and concomitantly increase conductivity [10,11]. Under these rules, the cellular structures, containing different permittivity, could be detected and differentiated under various frequencies. Low frequency with higher permittivity allows C_c to be detected and higher frequency promotes signal down into cytoplasm. Whether C_c or R_c in parallel with R_{SOL} will lead to a lower sensed resistance. Overall, based on the established model from Fig. 3, the entire channel impedance shows as:

$$Z_{Overall} = \frac{1}{\frac{1}{\left(R_C + \frac{2}{j\omega C_c}\right) \parallel R_{SOL} + Z_{CPE}} + j\omega C_{st}} \quad (1)$$

Channel resistance R_{SOL} is the targeted signal response whose variation is what the device wish to detect. At low frequency, C_{st} takes nearly no effect on the overall impedance while Z_{CPE} largely increases its magnitude, which obscures R_{SOL}. Also C_c dominates the cell-penetration impact on R_{SOL}. On the other hand, stray capacitance will reduce overall impedance as the frequency goes high, whereas hard to detect R_{SOL} and R_c we wish to differentiate from in each particles.

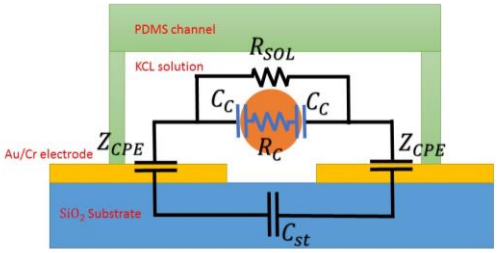

Fig. 3. Proposed/Modified Electrical Model for impedance spectroscopy.

C. Experimental Setup and Measurement

The frequency spectrum of the fabricated device is done by the MATLAB (MathWorks®) Simulation. For the chosen ideal frequency range, experiments initialize with implementation of fluorescence polystyrene beads (PolySciences, Inc.) into the microfluidic channel under the applied AC frequencies within the range. Existence of beads will be experimentally measured by employed lock-in amplifier (HF2LI, Zurich Instrument) which detects voltage differences. 1V is chosen as the input voltage since the higher causes unwanted electrolytic effects and the lower implies no signal response from the bead penetration. As for beads, 3, 6, 10um beads are simultaneously used to simulate real cell sizes such as erythrocytes, leukocytes or normal cells. We add 2% Pluronic F 108 Pastille (BASF SE®) as a surfactant to hydrophilize the polystyrene beads. The buffer liquid is 300mM potassium chloride whose conductivity lies in 1.5-1.7 S/m, suitable for entire experiment environments. For higher concentration, shielding effects from electrolytic electrodes will block the sensing mechanism while the lower will be hard to conduct. The overall experimental setup could be demonstrated as in Fig. 4.

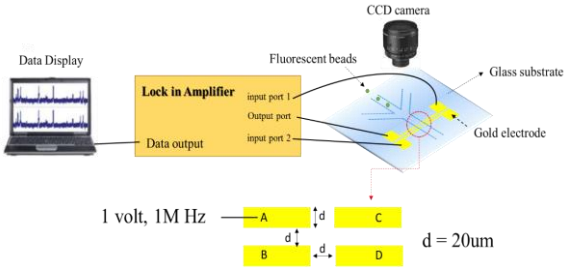

Fig. 4 The experimental setup for the particle-analyzing device.

An expected ideal operational frequency will be chosen from its maximum signal response at this frequency from experimental data under frequencies in the frequency range. This operational frequency will allow the following differentiation procedures when different positions and sizes of beads enter the channel.

D. Substrate Material Effect Test

To further understand the effect of stray capacitances (C_{st}), COMSOL Multiphysics software is used to simulate the entire device environment. The simulation calculates different charge density and rough stray capacitances in different substrate materials with a unique dielectric constant. Their capacitance effect will then be verified in the simulated impedance spectrum. Theoretically, a substrate material with higher dielectric constant implies better charge storage ability

which induces higher stray capacitance. Hence to alleviate C_{st} effects under high operational frequencies, we should apply substrate materials with lower dielectric constants. While parylene C and poly(methylmethacrylate) (PMMA) are both materials with lower dielectric constants, the fabrication process complicates with the parylene C coating layer on glass substrate compared to PMMA. Problems come when bad adhesive layers strip off in lift-off process when obtaining designed electrodes evaporated by Photolithography and e-gun evaporator. Moreover, bonding of the channel and parylene-coated substrate is hard to achieve with only O2 plasma treatment or reactive-ion etching where fabrication cost extremely goes high [12].

Instead, PMMA-coating substrate averts lift-off and bonding problems with a better adhesive property whether with glass substrate or PDMS channel. Therefore, in experiments, PMMA is then chosen to be tested as a new substrate material, expected to extend the frequency range to higher level. Fabrication processes are similar with those mentioned above except adding few more procedures. PMMA solution mixed with 5 % anisole are spin-coated on glass substrate and ready to be photoresist-coated with identical procedures mentioned before. For PMMA-PDMS bonding, RIE treatment is implemented with O2 50 sccm for 1min in power 100W. After the treatment, both parts are soaked into 5% (3-aminopropyl) triethoxysilane for 1min under 85 Celsius degrees. After then, they are bonded together for 2 hours under 65 Celsius degrees to bond neatly [13].

III. Result and Discussion

According to the developed-modified model, a simulated impedance spectrum is shown in Fig. 5. This result clearly shows the double layer impedance saliently blocks the detected signal at the frequency below 1 MHz and the parasitic behavior begins to intensely dominate the sensing impedance at the frequency higher than 15 MHz. As a consequence, the frequency spectrum of the fabricated device within 1 MHz to 15 MHz can be experimentally chosen as the optimal range for the bead detection process.

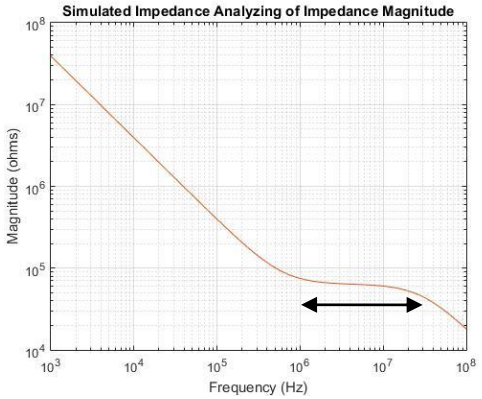

Fig. 5. Simulation of total analyzing impedance in channel from 1kHz to 100MHz without bead flow, where non-ideal capacitive effect is shown.

Within this frequency range, flowing 6um and 10um polystyrene beads are respectively detected by designed sensing electrodes with a syringe pump forwarding the beads into the channel. A sample of detected electrical across signal (electrode pair A-C) in Fig. 6a shows a set of high signal-to-noise ratio responses of measured output voltages. The peak value of an impedance response can be corresponded to the bead sizes and positions. Based on the individual results under each operational frequency, the frequency spectrum could be experimentally exemplified and correspond to the measured voltage differences in Fig. 6b. 1MHz-10MHz and 1MHz-15MHz operational frequency ranges for 6um and 10um respectively explicitly match the simulation results as the ideal impedance spectrum for our fabricated device.

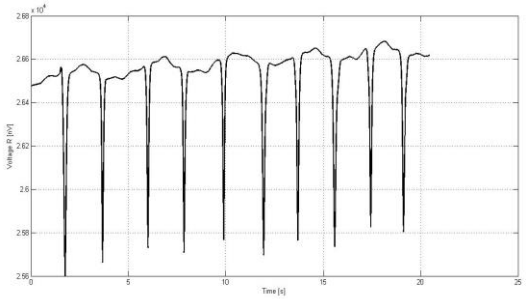

Fig. 6. (a) Sample of detected electrical across signal (electrode pair A-C) when beads flow upon sensing electrodes.

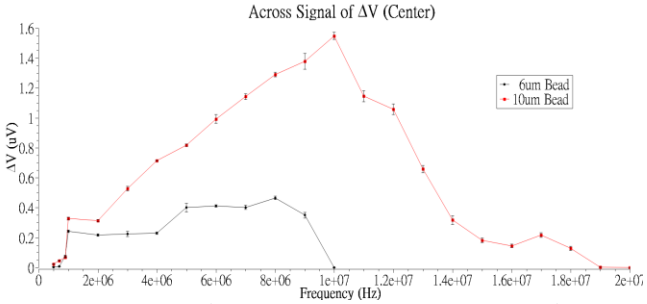

(b) Experimental results of △V caused by 6 um and 10um bead flows under frequency range specified in Fig. 5.

Size and Position information of various beads in channel is expected to obtain at low frequency which we choose as 1MHz based on measured voltage results in Fig. 4b. Employing the previous definitions of across and neighbor, the experimental peak-value distribution results at 1MHz can be shown as Fig. 7. 10um beads count for the largest responses to be differentiated from 6um and 3um beads. For position properties, beads of center position have better across signal responses and plain responses for neighbor signal while close position serve the

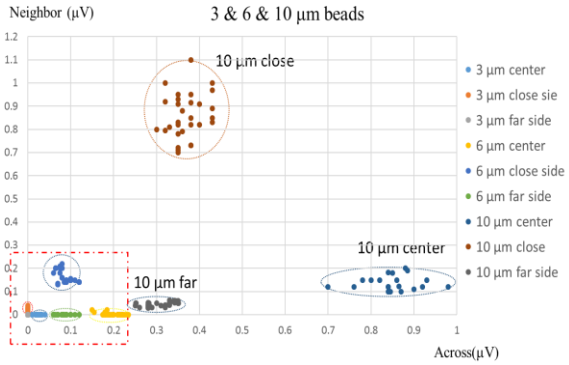

Fig. 7. (a) Organized data from peak responses of different sizes and positions of beads under 1MHz.

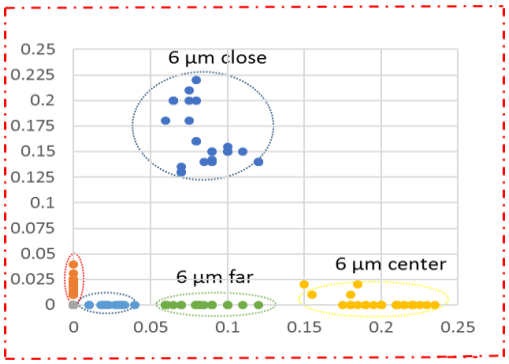

(b) Close look from part of (a).

opposite. The results are reasonable that beads in center disturb the electric field from electrode A to C most effectively and those in close from electrode A to B. Overall, it shows the experimental results successfully substantiate the fabricated device abilities for bead sizes and position differentiation.

For substrate effect test, COMSOL simulation result is performed in Fig. 8. Average Voltage Field and Charge density could be disclosed. With measured parameters, different stray capacitances of substrate materials are then calculated simultaneously and arranged in Table 1. In the results, a material with a higher dielectric constant indeed implies a higher stray capacitance which offers a narrower frequency range for detection. For PMMA and Parylene C, the calculated stray capacitance of them are a little above the half of that in glass. We could conclude that Parylene C and PMMA, with dielectric constant lower than glass, are ideally for substrate material selection to minimize the non-ideal capacitance effect. More experiments will verify the hypothesis by proffering a substantial set of data.

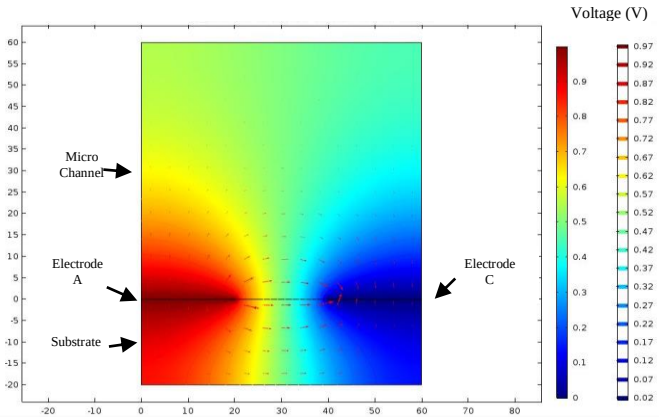

Fig. 8. Simulation under COMSOL tools of electrical field distribution in the channel cross section and glass substrate where stray capacitances are calculated.

TABLE I
COMPARISON OF SUBSTRATE MATERIAL SIMULATED INFLUENCE AT 10MHZ

Parameter	Material				
	Glass (SiO2)	PMMA	Parylene C	Polyimide	Nitride
Dielectric const. (at 1MHz)	4.2	2.6	2.95	3.9	7.5
Ave Voltage Field (V)	0.4995	0.4995	0.4995	0.4995	0.4995
Charge Density (10^{-4} C/m^2)	2.20	1.37	1.55	2.05	3.94
Rough C_{st} (pF)	0.53	0.33	0.37	0.49	0.95

Their effect on the impedance spectrum could be further illustrated under simulation in Fig. 9. Except for Nitride with relatively large dielectric constant, the impedance spectrum remains similar under 10MHz. However, stray capacitance effect could influence the overall channel impedance if we apply different substrate materials above 10MHz. PMMA and Parylene C has extended the range of flat impedance spectroscopy compared to glass as shown in Fig. 9. We could see the stray capacitance effect is mitigated where it starts to influence the signal response above 12-13MHz. Numerically, the impedance magnitude slope of PMMA-coated device and Parylene-coated device are approximately $-3.28\text{x}10^{-4}$ and $-3.98\text{x}10^{-4}$ at 12MHz compared to $-7\text{x}10^{-4}$ of glass. It implies its ability to mitigate stray capacitance statistically twice stronger than the original device.

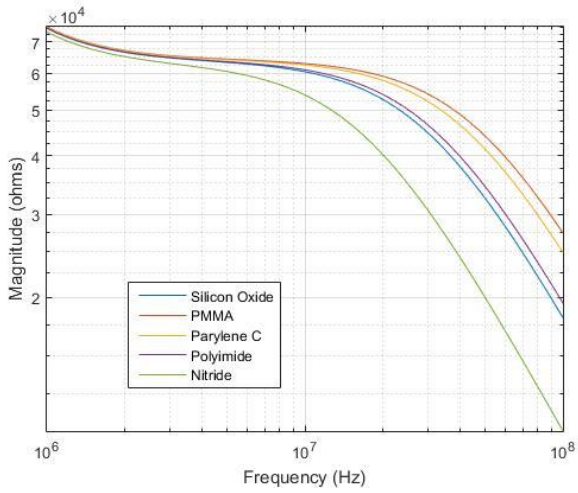

Fig. 9. Simulated Bode plot for channel impedance magnitude based on model with substrate materials of varying C_{st} calculated in COMSOL tools.

To verify the substrate material selection impact on the frequency spectrum, 6 um polystyrene beads are experimentally injected into the microchannel of devices with PMMA-coated substrate. Since Fig. 9 indicates the difference of impedance spectroscopy from different substrate materials approximately start from 6MHz, experimental results of △V caused by 6 um bead flows above 6MHz in these two devices compared with the original one are shown in Fig. 10.

At 9MHz, PMMA-coated device shows a voltage difference of 0.165uV compared to 0.06uV of original device. Also it allows signal response 0.04uV to be sensed at 12MHz. Thus, we could conclude clearly that the device with the original glass substrate allows maximum sensing frequency up to 9MHz while PMMA extends its ability to 12MHz. Subsequently, it simultaneously corresponds to Fig. 9. where the stray capacitance effect starts to impact above 12MHz in PMMA-coated device. The theory is verified that a 2MHz sensing range is created with PMMA-coated device whether shown in simulated impedance spectrum or experimental data. Moreover, better signal response magnitudes compared to glass substrate could be obtained using PMMA as substrate materials. Finally, it substantiates that substrate with lower dielectric constant mitigates the stray capacitance effect and gives out a better sensing environment above 10MHz.

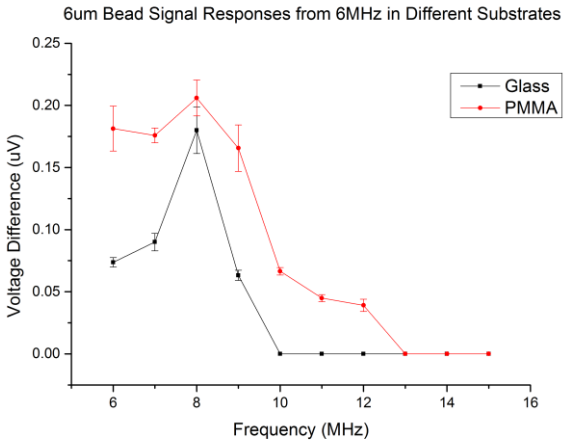

Fig. 10. Signal Responses when 6um beads are injected into microchannels on a PMMA-coating substrate and a glass substrate.

IV. Conclusions

Microfluidic electrical impedance cytometry provides a low-cost point of care device to discriminate cells. In this work, we present a new fabricated device for advanced particle analyzing where 4 coplanar electrodes are designed. An impedance spectrum is simulated and experimentally verified to have found an optimal frequency range 1MHz-15MHz for detecting beads. Then, an operational frequency 1MHz has been chosen to successfully discriminate particle properties such as sizes and positions which indicates the device's capability of becoming an effective electrical impedance analyzing tool. Further, the stray capacitance effect at high frequency is shown and mitigated by substrate material selection. Thus, it is important to employ different substrate materials for multi-frequency spectrum analysis. Utilizing poly(methylmethacrylate) (PMMA), the analysis with higher frequency range could demonstrate more cell intracellular characteristics while using this low-cost point-of-care device.

Acknowledgment

The authors are grateful to NTU Nano-BioMEMS Group and NTU Ultrasonic Imaging Lab. All microfabrication was done in NTU Graduate Institute of Electronics Engineering.

References

[1] S. Gawad, L. Schild and P. Renaud, "Micromachined impedance spectroscopy flow cytometer for cell analysis and particle sizing," *Lab on a Chip*, 1, 76-82, 2001.

[2] K. Cheung, S. Gawad, and P. Renaud, "Impedance Spectroscopy Flow Cytometry: On-Chip Label-Free Cell Differentiation," *Cytometry. Part A*, 65A, 124-132, 2005.

[3] D. Spencer and H. Morgan, "Positional dependence of particles in microfluidic impedance cytometry," *Lab on a Chip*, 11, 1234-1239, 2011.

[4] H. E. Ayliffe, A. B. Frazier, and R. D. Rabbitt, *Journal of MEMS*, vol. 8, pp. 50-57, 1999.

[5] S. Zheng and Y.-C. Tai, "Human Blood Cell Sensing with Platinum Black Electroplated Impedance Sensor," *IEEE-NEMS'07*: Bangkok, Thailand, 2007.

[6] T.-W. Wu, C.-H. Kao, and C.-T. Lin, "A Microfluidic Cell Counting Device Based on Impedance Analysis," *16th International Meeting on Chemical Sensors*, Jeju, Korea, Jul. 2016.

[7] J.-L. Hong, and K.-C. Lan, "Electrical characteristics analysis of various cancer cells using a microfluidic device based on single-cell impedance measurement," *Sensors and Actuators B*: *Chemical*, 173, 927-934, 2012.

[8] D. Satake, H. Ebi, N. Oku, K. Matsuda, H. Takao, M. Ashiki, and M. Ishida, "A sensor for blood cell counter using MEMS technology," *Sensors and Actuators B: Chemical*, vol. 83, pp. 77, 2002.

[9] J. H. Nieuwenhuis, F. Kohl, J. Bastemeijer, P. M. Sarro, and M. J. Vellekoop, "Integrated Coulter counter based on 2-dimensional liquid aperture control," *Sensors and Actuators B: Chemical*, vol. 102, pp. 44, 2004.

[10] G. H. Markx and C. L. Davey, "The dielectric properties of biological cells at radiofrequencies: Applications in biotechnology," *Enzyme and Microbial Technology*, 25, 161-171, 1999.

[11] Khalil Heileman, Jamal Daoud and Maryam Tabrizian, "Dielectric spectroscopy as a viable biosensing tool for cell and tissue characerization and analysis," *Biosensors and Bioelectronics*, 49, 348-359, 2013.

[12] Pouya Rezai, P Ravi Selvaganapathy and Gregory R Wohl, "Plasma enhanced bonding of polydimethylsiloxane with parylene and its optimization," *Journal of Micromechanics and Microengineering*, 21, pp 13, 2011.

[13] Kangil Kin, Sin Wook Park and Sang Sik Yang, "The optimization of PDMS-PMMAbonding process using silane primer," *BioCihp*, 4(2): 148-154, 2010.